Journal of Nuclear Materials 514 (2019) 109–113

Contents lists available at ScienceDirect

Journal of Nuclear Materials

journal homepage: www.elsevier.com/locate/jnucmat

Deuterium plasma driven permeation behavior in a Chinese reduced activation martensitic/ferritic steel CLF-1

Hao-Dong Liu [a, b], Hai-Shan Zhou [a, *], Yu-Ping Xu [a], Yi-Ming Lyu [a, b], Lu Wang [a, b], Fang Ding [a], Guang-Nan Luo [a, b]

[a] Institute of Plasma Physics, Chinese Academy of Sciences, Hefei, Anhui, 230031, China
[b] Science Island Branch of Graduate School, University of Science and Technology of China, Hefei, Anhui, 230031, China

ARTICLE INFO

Article history:
Received 3 March 2018
Received in revised form
18 September 2018
Accepted 7 November 2018
Available online 12 November 2018

Keywords:
Hydrogen isotope
Plasma driven permeation
RAFM steel

ABSTRACT

Deuterium (D) plasma-driven permeation (PDP) experiments for a Chinese reduced activation martensitic/ferritic steel CLF-1 have been performed. The effects of implantation flux, sample temperature and ion incident energy have been studied. The steady state PDP flux is found to be proportional to the square root of the implantation flux, indicating that the permeation takes place in recombination-limited regime for the upstream surface and diffusion-limited regime for the downstream surface (RD). The PDP flux and flux ratio (PDP flux/implantation flux) decrease with the increase of ion incident energy, which may be due to the enhancement of D recombination coefficient at the upstream surface.

1. Introduction

Fusion blanket structural materials will be subjected to 14 MeV fusion neutrons. The austenitic stainless steel is not suitable for DEMO reactor due to its irradiation swelling at high doses. Therefore, the concept of reduced activation ferritic/martensitic (RAFM) steels was proposed based on the composition of high Cr heat resistant steels, Mod 9Cr–1Mo (Grade91, ASME Section II), by replacing Mo with W and Nb with Ta to meet the shallow land burial limitation, known for their excellent high dose irradiation swelling resistance [1]. RAFM steels are considered to be the most promising candidate structure material for a fusion reactor.

China is implementing its ITER testing blanket module (TBM) program. A helium-cooled ceramic breeder (HCCB) concept has been selected for Chinese TBM [2]. Based on the requirement of ITER TBM program and Chinese development strategy for fusion DEMO, a RAFM steel named CLF-1 has been developed as the structural material [3]. One of the major testing objectives of Chinese TBM is to validate tritium breeding capability of the HCCB concept [4]. However, tritium transport through the first wall into the breeding area by plasma driven permeation (PDP) may introduce additional tritium and affect the evaluation of tritium production efficiency. As a result, understanding tritium plasma driven permeation through RAFM steel is essential for the precise tritium production assessment.

In this work, deuterium (D) plasma driven permeation through CLF-1 steel experiments were performed. The effects of implantation flux, sample temperature and ion incident energy have been studied. A key transport parameter, i.e. the surface recombination coefficient, has been evaluated under various plasma conditions as well [5].

2. Experimental

CLF-1 steel [6], developed by Southwestern Institute of Physics (SWIP) was used as the specimen in this experiment. Disks with a diameter of 48 mm are used for the plasma driven permeation experiment. The effective permeation diameter of the sample is 35 mm. Both sides of samples were first mechanically polished using SiC abrasive paper up to #2000 with water cooling and then mechanically polishing with diamond powder to a mirror finish, ultrasonically cleaned in alcohol to remove the polishing residuals and outgassed at 723 K for 2 h. The detailed chemical composition of CLF-1 steel are listed in Table 1.

X-ray photoelectron spectroscopy (XPS) (ESCA1600 system, ULVAC-PHI Inc.) was utilized to evaluate the surface conditions

* Corresponding author. Institute of Plasma Physics, Chinese Academy of Sciences, Hefei, Anhui, 230031, China.
E-mail address: haishanzhou@ipp.ac.cn (H.-S. Zhou).

https://doi.org/10.1016/j.jnucmat.2018.11.012
0022-3115/

Table 1
The chemical composition of the CLF-1 steel [6].

Element	Cr	W	Ta	V	C	Mn	Fe
wt.%	8.5	1.5	0.10	0.25	0.11	0.51	Balance

with different sputtering times (0 s, 5 s and 30 s). 3 keV Ar ion herein was used for the sputtering.

The schematic diagram of the PDP setup in a laboratory-scale linear plasma device: Permeation and Retention Evaluation FACility for fusion Experiments (PREFACE) [7] at the Institute of Plasma Physics, Chinese Academy of Sciences, is shown in Fig. 1. PREFACE facility is equipped with a 2.45 GHz microwave source with maximum power of 2 kW. The vacuum discharge chamber is isolated by a ceramic window (Al_2O_3) from the microwave system. The chamber is evacuated by a turbo molecular pump. Four water cooling solenoidal winding magnets provide a magnetic field of 875 Gs for ECR plasma discharge. A Hiden Langmuir probe (ESPion) is employed to measure the plasma density and electron temperature. A tungsten filament heater is used to raise the sample temperature, which can be recorded by a K-type thermocouple tightly pressed onto the specimen. In the present study, ~0.6 Pa D_2 gas is introduced into the main chamber to produce D plasma. The base pressure of the downstream side is 7.2×10^{-5} Pa. The PDP flux is detected by a Pfeiffer QMG 422 quadrupole mass spectrometer (QMS). The QMS is calibrated by a D_2 standard leak provided by Vacuum Technology Incorporated (VTI). The leak rate is 9.71×10^{-6} atm-cc/s.

3. Theory

There are three transport regimes for hydrogen atoms implanted into solid under the influence of diffusion and surface recombination [5]: (1) diffusion-limited release of hydrogen from both surfaces (DD-regime); (2) recombination-limited release of hydrogen from the upstream surface and diffusion-limited release of hydrogen from the downstream surface (RD-regime); (3) recombination-limited release of hydrogen for both surfaces (RR-regime). The three regimes could be distinguished from three dimensionless parameters W, α and γ. This model was used to analyses the hydrogen permeation behavior for F82H [8] and tungsten [9].

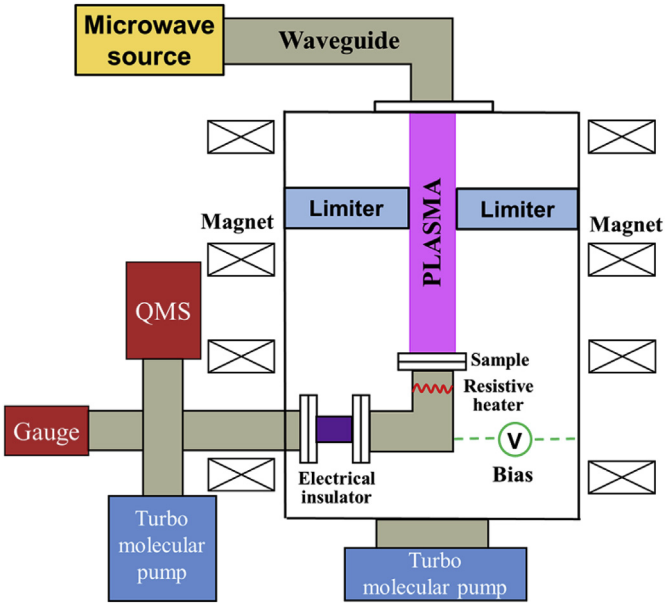

Fig. 1. The schematic diagram of plasma-driven permeation setup in PREFACE.

$$W = \frac{R\sqrt{J_i K_{up}}}{D} \tag{1}$$

$$\alpha = \frac{R}{L} \tag{2}$$

$$\gamma = \sqrt{\frac{K_{up}}{K_{dn}}} \tag{3}$$

Where R represents the ion projected range, J_i denotes the implantation flux, D represents the bulk diffusion coefficient, L is the sample thickness, K_{up} is the upstream surface recombination coefficient, K_{dn} is the downstream surface recombination coefficient.

$W > 1$, DD – regime;

$\gamma^2\alpha < W < 1$, RD – regime;

$W < \gamma^2\alpha$, RR – regime.

In different regimes, the steady-state PDP flux J_p could be expressed as:

$$\text{DD} - \text{regime}\quad J_p = \frac{R}{L}J_i \tag{4}$$

$$\text{RD} - \text{regime}\quad J_p = \frac{D}{L}\sqrt{\frac{J_i}{K_{up}}} \tag{5}$$

$$\text{RR} - \text{regime}\quad J_p = \frac{K_{up}}{K_{up}+K_{dn}}J_i \tag{6}$$

Only in RD-regime, the steady-state PDP flux J_p should be proportional to the square root of the implantation flux. We could also obtain the upstream surface recombination coefficient K_{up} through the steady-state PDP flux J_p measured by PDP experiment with the following equation:

$$K_{up} = \frac{D^2 J_i}{L^2 J_p^2} \tag{7}$$

4. Results and discussion

4.1. Implantation flux dependence of PDP flux

Fig. 2 shows the PDP fluxes through 0.75 mm thick CLF-1 steel with different microwave input powers. In this experiment, the sample is preheated at 586 K. Then the plasma is ignited and the plasma flux increases with the increase of the microwave input power. In the whole experiment, the sample temperature remains the same.

The PDP flux for CLF-1 is initially a sudden (~30 s) and drastically enhanced permeation followed by a decay to lower steady-state values, which is called “transient peak” region. Nevertheless, the transient peak region is not evident in the next larger implantation flux. The initial transient peak and the following gentle peak with the same implantation flux has been observed by other researchers [10]. XPS results shown in Fig. 3 indicate that the sample surface is

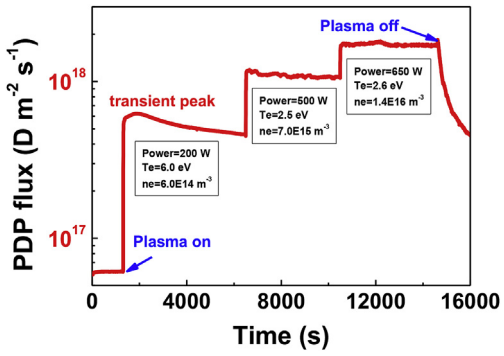

Fig. 2. D PDP behavior for 0.75 mm thick CLF-1 steel with different microwave input powers.

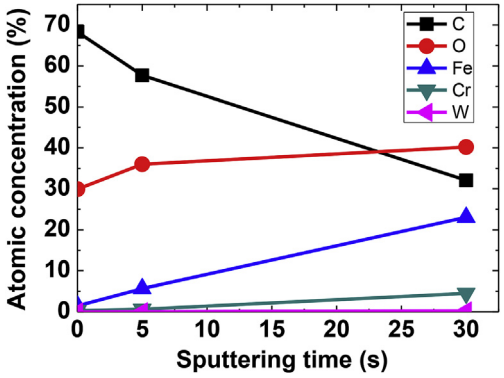

Fig. 3. XPS results for the surface with different sputtering time using Ar ion.

usually covered with native layers of oxygen (O) and carbon (C) non-metallic impurities. With the sputtering time increasing, the C atom concentration decreases significantly, O atom concentration increases slightly and the substrate atom (Fe, Cr and W) concentrations increase. These surface layers retard the recombination of the emerging D at the upstream (implantation) surface causing a significant fraction of the implanted D to diffuse to and escape from the downstream surface. During plasma exposure, the surface layers would be sputtered away from the surface by the energetic particles, when the particle energy is higher than the threshold energy of the surface layers. Most of these layers could be removed in a short time, but some oxygen cannot be excluded [11]. The time for the peak to decay corresponds with the time for removal of surface oxides and surface deposits of segregated constituents [10]. The transient peak could be attributed to the recombination coefficient increasing with time due to the removal of impurities [12].

The implantation flux into a membrane is calculated from equation (10) [8]:

$$J_i = \sum_{j=1}^{3} \frac{(1-R_j)jN_j}{2} \sqrt{\frac{k_B(T_e+T_i)}{m_{D_j^+}}} \tag{10}$$

R_j is the reflection coefficient of ion D_j^+ from IPP report [13], N_j is the density of ion D_j^+, k_B is the Boltzmann constant, T_e and T_i ($T_i \approx 0$) are the electron and ion temperatures, m is the ion mass. The density ratio of D ion species is estimated by Refs. [8,14].

Shown in Fig. 4 are the D permeation data taken from PDP experiments at the surface temperature of 586 K. The PDP flux increases with the increase of the implantation flux. Equation (5) means that the PDP flux is proportional to the square root of the implantation flux in RD-regime. Thereby, the theoretical value of

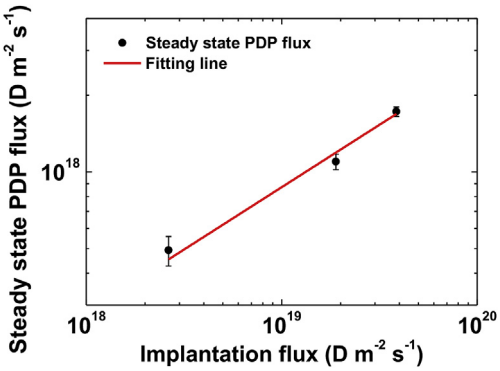

Fig. 4. D implantation flux dependence of PDP flux.

the log-log relationship between the PDP flux and the implantation flux in RD-regime is 0.50. The slope of the experimental fitting line is 0.47, which agrees well with the theoretical value, indicating that permeation takes place in the RD-regime.

Fig. 5 shows that the relationship between the D steady state PDP flux ratio and the implantation flux at the temperature of 586 K. The slope of the fitting line is −0.53. The D steady state PDP flux ratio decreases with the increase of the implantation flux. The relationship between the steady state PDP flux ratio and the implantation flux should be decided by Equation (11) derived from equation (5). Equation (11) could be rewritten as equation (12) in log-log coordinate. Generally, the diffusion coefficient D and recombination coefficient K_{up} obey the Arrhenius equation. D and K_{up} are constants at a fixed temperature. The theoretical value of the slope of the fitting line should be −0.5. As a result, the PDP flux ratio should be decreased with the implantation flux increasing only in RD-regime. In DD (equation (13)) or RR (equation (14)) regime, the PDP flux ratio should be a constant at a fixed temperature.

$$\frac{J_p}{J_i} = \frac{D}{L\sqrt{K_{up}}} \cdot \frac{1}{\sqrt{J_i}} \tag{11}$$

$$\log\left(\frac{J_p}{J_i}\right) = -0.5 \cdot \log J_i + \log\left(\frac{D}{L\sqrt{K_{up}}}\right) \tag{12}$$

$$\frac{J_p}{J_i} = \frac{R}{L} \tag{13}$$

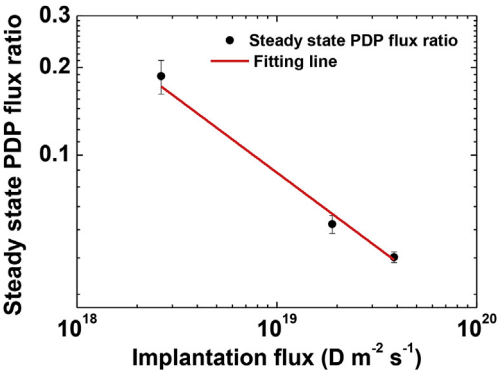

Fig. 5. D plasma implantation flux dependence of steady state PDP flux ratio.

$$\frac{J_p}{J_i} = \frac{K_{up}}{K_{up} + K_{dn}} \tag{14}$$

4.2. Sample temperature and ion incident energy dependence of PDP flux

Different negative bias voltages on the sample were applied to increase the ion incident energy on the sample. The experimental bias voltage was performed from 0 V increasing to −100 V. The ion flux increased with the bias voltages. The measured electron temperature and electron density for 0 V, −50 V and −100 V were Te = 2.0 eV, 2.7eV and 3.0 eV, ne = 5.0×10^{16}, 5.1×10^{16} and 5.5×10^{16} m^{-3}. The ion flux were 2.44×10^{20}, 2.89×10^{20} and 3.29×10^{20} $D\cdot m^{-2}\cdot s^{-1}$ for 0 V, −50 V and −100 V, respectively. Fig. 6 shows the ion distribution ranges of D implanted in the CLF-1 target calculated by SRIM code. The ion incident energy for the sample without a bias voltage calculated from $e(V_p - V_f)$, e is the elementary electron charge, V_f is the floating potential (+1 V), V_p is the plasma space potential (+8 V). For the sample with a bias voltage V_b, the ion incident energy is $e(V_b - V_p)$. The ion projected ranges are 0.55 nm, 1.85 nm and 2.70 nm for the different negative bias voltages of 0, -50 V and −100 V, respectively. The corresponding values of α are 7.40×10^{-7}, 2.47×10^{-6} and 3.60×10^{-6}, respectively.

Fig. 7 shows the steady state PDP flux ratio applied with different bias voltages verse sample temperature for CLF-1. The PDP flux ratio increases with the increase of the temperature but decreases with the increase of the ion incident energy.

It is worthwhile to remark that if we increase the ion incident energy by applying a negative bias on the sample, the implantation flux and the sample temperature increase immediately, however, the PDP flux decreases immediately. If we only increase the sample temperature by increasing the sample heating power, the PDP flux increases. In accordance with Fig. 4, if we only increase the implantation flux, the PDP flux increases. Thus, the recombination coefficient should increase more compared with other parameters in the case of higher ion incident energy according to equation (7). The D recombination coefficients for CLF-1 steel applied with different negative bias voltages are shown in Fig. 8. The recombination coefficient decreases at elevated temperatures. The recombination coefficient in the case of the higher ion incident energy is higher than that in the case of the lower ion incident energy. This may be attributed to a cleaner surface because of the higher capacity of removal of surface contaminants with higher ion incident energy. In addition, 50 eV is higher than the threshold energy for D sputtering of iron [15]. The sputtering of iron should also affect the surface conditioning and then affect the D recombination on the surface. The recombination coefficient for F82H in the case of hydrogen plasma with a negative bias of −100 V [16] is less than that for CLF-1 in the case of D plasma with a negative bias of −100 V. This could be attributed to the lighter ion mass.

In the case of low energy ion and ~mm thick RAFM steel, the ion injection depth is very shallow (~nm), α is very small (~1×10^{-6}). The rate-determining step at the upstream side should be the recombination process and the release of hydrogen from the downstream surface should be diffusion-limited (i.e. RD-regime). When the ion incident energy is high enough, RD-regime may turn into DD regime. In order to determine this, the transport parameter, W, is plotted as function of inverse temperature shown in Fig. 9. W decreases with the increase of the temperature and

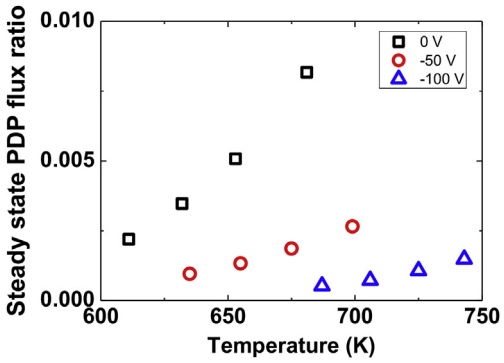

Fig. 7. Steady state PDP flux ratio verse temperature for CLF-1.

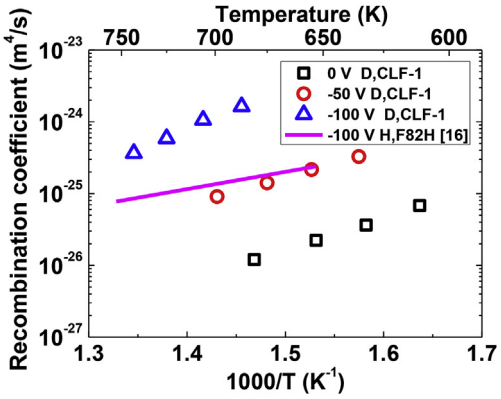

Fig. 8. D recombination coefficient for CLF-1 steel.

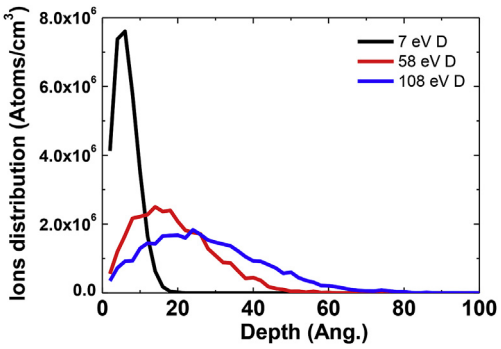

Fig. 6. Ion distribution ranges of D implanted in the CLF-1 target by SRIM code.

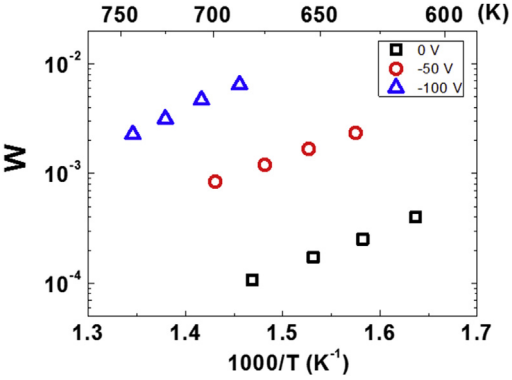

Fig. 9. Transport parameter, W, for CLF-1 steel.

increases with the increase of ion incident energy but always less than one in the experimental temperature range and bias voltage range. It indicates the ion incident energy is not high enough to make the PDP behavior controlled by DD regime.

5. Conclusion

The PDP behavior through ~ mm thickness RAFM steel is controlled by RD regime. The PDP flux increases but the steady state PDP flux ratio decreases with the increase of the implantation flux. The PDP flux is sensitive to the surface conditioning. The surface exposed to plasma is of major importance. Generally, the native surface impurity layers enhance the permeation. The PDP flux reduces along with the surface layer sputtered by plasma bombardment. The higher ion incident energy means the higher capacity of removal of surface contaminants and sputtering. The surface conditioning in the case of higher ion incident energy makes the D recombination coefficient increase, the PDP flux decrease and the steady state PDP flux ratio decrease.

In addition, there are always some impurities (H_2O, CO, CH_4 and other organic species) in the fusion reactors [17], which could also redeposit on the surface of PFM and may increase the hydrogen isotope permeation. The high energy particle could sputter the surface layer and even PFM subtrate atoms away from the surface and reduce the hydrogen isotope permeation at the same time. Hence, the permeation is a dynamic variation process dependent of the surface condition. In order to get the accurate tritium breeding ratio (TBR) in ITER TBM program, it is quite important to measure the particle (atom, ion, molecular) species, flux and incident energy, which need more work on this subject.

Acknowledgments

The authors would like to thank Profs. K.-M. Feng and Y.-J. Feng for providing the CLF-1 steel. The authors also thank Prof. Yasuhisa Oya for the XPS measurement. This work is supported by the National Natural Science Foundation of China (No. 11505232), the National Magnetic Confinement Fusion Science Program of China (No.2015GB109001), the Science Foundation of Institute of Plasma Physics, Chinese Academy of Sciences (No. DSJJ-16-JC01) and the China Postdoctoral Science Foundation (Nos. BX201700248, 2017M622035).

References

[1] H. Tanigawa, E. Gaganidze, T. Hirose, M. Ando, S. Zinkle, R. Lindau, E. Diegele, Development of benchmark reduced activation ferritic/martensitic steels for fusion energy applications, Nucl. Fusion 57 (2017) 092004.
[2] K. Feng, C. Pan, G. Zhang, T. Luo, Z. Zhao, Y. Chen, X. Ye, G. Hu, P. Wang, T. Yuan, Progress on solid breeder TBM at SWIP, Fusion Eng. Des. 85 (10) (2010) 2132–2140.
[3] P. Wang, J. Chen, H. Fu, S. Liu, X. Li, Z. Xu, Technical issues for the fabrication of a CN-HCCB-TBM based on RAFM steel CLF-1, Plasma Sci. Technol. 15 (2) (2013) 133.
[4] L.M. Giancarli, M. Abdou, D.J. Campbell, V.A. Chuyanov, M.Y. Ahn, M. Enoeda, C. Pan, Y. Poitevin, E. Rajendra Kumar, I. Ricapito, Y. Strebkov, S. Suzuki, P.C. Wong, M. Zmitko, Overview of the ITER TBM program, Fusion Eng. Des. 87 (5) (2012) 395–402.
[5] B.L. Doyle, A simple theory for maximum h inventory and release: a new transport parameter, J. Nucl. Mater. 111 (1982) 628–635.
[6] P. Wang, J. Chen, H. Fu, S. Liu, X. Li, Z. Xu, Effect of N on the precipitation behaviours of the reduced activation ferritic/martensitic steel CLF-1 after thermal ageing, J. Nucl. Mater. 442 (1–3) (2013) S9–S12. Supplement 1.
[7] H.S. Zhou, H.D. Liu, Z.Q. An, B. Li, Y.P. Xu, F. Liu, M.Z. Zhao, Q. Xu, F. Ding, G.N. Luo, Deuterium permeation and retention in copper alloys, J. Nucl. Mater. 493 (2017) 398–403.
[8] H. Zhou, Y. Hirooka, N. Ashikawa, T. Muroga, A. Sagara, Hydrogen plasma-driven permeation through a reduced activation ferritic steel alloy F82H, Fusion Sci. Technol. 63 (1T) (2013) 361–363.
[9] H.T. Lee, H. Tanaka, Y. Ohtsuka, Y. Ueda, Ion-driven permeation of deuterium through tungsten under simultaneous helium and deuterium irradiation, J. Nucl. Mater. 415 (1) (2011) S696–S700. Supplement.
[10] G. Longhurst, R. Anderl, D. Struttmann, A comparison of implantation-driven permeation characteristics of fusion reactor structural materials, J. Nucl. Mater. 141 (1986) 229–233.
[11] M. Mayer, A. Kleyn, P.Z. van Emmichoven, Strongly reduced penetration of atomic deuterium in radiation-damaged tungsten, Phys. Rev. Lett. 111 (22) (2013) 225001.
[12] R.A. Anderl, D.F. Holland, G.R. Longhurst, Hydrogen transport behavior of metal coatings for plasma-facing components, J. Nucl. Mater. 176 (1990) 683–689.
[13] W. Eckstein, IPP Report 9/132, Max-Planck-Institut für Plasmaphysik, Garching, Germany, 2002.
[14] E. Hollmann, A.Y. Pigarov, Measurement and modeling of molecular ion concentrations in a hydrogen reflex-arc discharge, Phys. Plasmas 9 (10) (2002) 4330–4339.
[15] Y. Yamamura, H. Tawara, Energy dependence of ion-induced sputtering yields from monatomic solids at normal incidence, Atomic Data Nucl. Data Tables 62 (2) (1996) 149–253.
[16] H. Zhou, Y. Hirooka, N. Ashikawa, T. Muroga, A. Sagara, Gas- and plasma-driven hydrogen permeation through a reduced activation ferritic steel alloy F82H, J. Nucl. Mater. 455 (1–3) (2014) 470–474.
[17] M.E. Notkin, A.I. Livshits, A.M. Bruneteau, M. Bacal, Effect of ion bombardment on plasma-driven superpermeation of hydrogen isotopes through a niobium membrane, Nucl. Instrum. Methods Phys. Res. Sect. B Beam Interact. Mater. Atoms 179 (3) (2001) 373–382.